Internal noise and system size effects induce nondiffusive kink dynamics

Diego A. C. Contreras* and Marcel G. Clerc†

Departamento de Física, Facultad de Ciencias Físicas y Matemáticas, Universidad de Chile, Casilla 487-3, Santiago, Chile

(Received 12 January 2015; published 23 March 2015)

We investigate the effects of inherent fluctuations and system size in the dynamics of domain between uniform symmetric states. In the case of monotonous kinks, this dynamics is characterized by exhibiting nonsymmetric random walks, being attracted to the system borders. For nonmonotonous interface, the dynamics is replaced by a hopping dynamic. Based on bistable universal models, we characterize the origin of these unexpected dynamics through use of the stochastic kinematic laws for the interface position and the survival probability. Numerical simulations show a quite good agreement with the theoretical predictions.

DOI: 10.1103/PhysRevE.91.032922 PACS number(s): 05.45.−a, 05.10.Gg, 05.40.Ca

I. INTRODUCTION

Macroscopic systems under the influence of injection and dissipation of quantities such as energy and momenta usually exhibit coexistence of different states—this feature is usually denominated multistability [1]. This is clearly a manifestation that far from equilibrium systems are of nonlinear nature. Heterogeneous initial conditions usually caused by the inherent fluctuations generate spatial domains, which are separated by their respective interfaces. These interfaces are known as front solutions or interfaces, or domain walls [2–4]. Interfaces between these metastable states appear in the form of propagating fronts and give rise to rich spatiotemporal dynamics [5–7]. Front dynamics occurs in systems as different as walls separating magnetic domains [8], directed solidification processes [9], nonlinear optical systems [10,11,13,33], oscillating chemical reactions [14], fluidized granular media [15–21], and population dynamics [22–24], to mention a few. From the point of view of dynamical systems theory, in one spatial dimension a front is a nonlinear solution that is identified in the comoving frame system as a heteroclinic orbit linking two spatially extended uniform states [25,26]. The evolution of front solutions can be regarded as a particle-type one, i.e., they can be characterized by a set of continuous parameters such as position, core width, and so forth.

The interface dynamics depends on the nature of the states that are connected. In the case of a front connecting a stable and an unstable state, it is usually called a Fisher-Kolmogorov-Petrosvky-Piskunov (FKPP) front [22,27,28]. One of the characteristic features of these fronts is that their speed is not unique, but determined by the initial conditions. When the initial condition is bounded, after a transient, two counterpropagative fronts with the minimum asymptotic speed emerge [22,28]. FKPP fronts have been observed in Taylor-Couette [29], Rayleigh-Benard experiments [30], pearling and pinching on the propagating Rayleigh instability [31], spinodal decomposition in polymer mixtures [32], and liquid crystal light valves [33], to mention a few.

The former scenario changes drastically for a front connecting two stable uniform states. In this case, a variational system tends to develop the most stable state, in order to minimize its energy or Lyapunov function, so that the front always propagates towards the most energetically unfavorable state. There is only one point in the parameter space for which the front is motionless, which is commonly called the Maxwell point and is the point for which the two states have exactly the same energy [34]. Close to the Maxwell point, based on the parameters variation method, one can analytically determine the front speed [5]. For variational systems away from the Maxwell point one can have implicit expressions for the front speed [5], which correspond to nonlinear eigenvalue problems. In the nonvariational case, the analytical expression of the front speed is a problem still unresolved.

Systems with discrete reflection symmetries can possess two equivalent uniform states with interfaces, or domain walls, which are generically at rest. Indeed, the two connected states are energetically equivalent. These front solutions are termed kinks. However, under spontaneous breaking of the parity symmetry, these fronts can acquire a nonzero asymptotic speed. This phenomenon is denominated the nonvariational Ising-Bloch transition [35]. Variational systems do not exhibit this phenomenon, because the front speed is proportional to the energy difference between the two equivalent states.

On the other hand, a characteristic property of macroscopic systems is to present incoherent and uncontrollable fluctuations, as a result of their microscopic constituents. When macroscopic fluctuations are not dependent on the macroscopic variables describing the system is called internal or additive noise, in the opposite case, it is called external or multiplicative noise. Usually, the effects of these fluctuations were either considered as a nuisance (degradation of the signal-to-noise ratio) or ignored because it was not known how to handle them. In recent decades, a wealth of theoretical and experimental research has shown that fluctuations can have rather surprisingly constructive and counterintuitive effects in many physical systems, and that they can be figured out with the help of different analysis tools. These situations occur when there are mechanisms of noise amplification, or when noise interacts with nonlinearities or driving forces on the system. The most well-know examples in zero-dimensional systems are noise-induced transition [36] and stochastic resonance [37]. More recently, examples in spatially extended system are noise-induced phase transition, noise-induced patterns (see Ref. [38] and references therein),

*diegocc@ug.uchile.cl
†marcel@dfi.uchile.cl

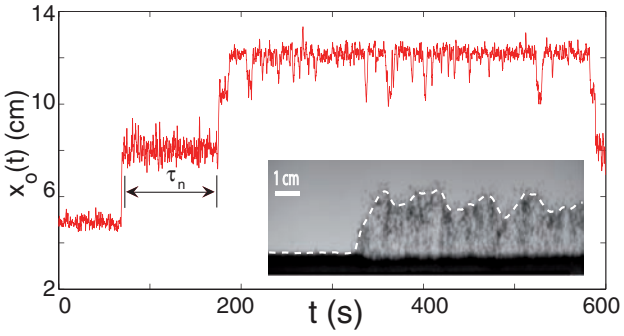

FIG. 1. (Color online) Temporal evolution of a granular kink position, x_0, in a shallow one-dimensional fluidized granular layer subjected to a periodic air flow [45]. The inset snapshot corresponds to a granular kink observed at a given moment.

noise-sustained structures in convective instability [39], stochastic spatiotemporal intermittency [40], precursor of patterns [41], noise-induced traveling waves [42], noise-induced ordering transition [43], and front propagation [44]. A natural question that arises is what is the effect of internal fluctuations on kink dynamics. As we have mentioned before, these extended solutions can be described as particle-type solutions. Hence, one expects that the effect of the inherent fluctuations induces a Brownian particle for the kink position (see Ref. [38] and references therein). Recently in Refs. [20,21], observations of kinks in a shallow one-dimensional fluidized granular layer subjected to a periodic air flow were reported each domain varied periodically with half of the forcing period. Figure 1 shows a granular kink observed at a given moment and the respective dynamic evolution of the kink position. Due to the internal fluctuations of the granular bed, the kink profile exhibits an effective wavelength, a precursor, which modulates spatially the homogeneous states and drastically modifies the kink dynamic. Indeed, it is shown that the temporal evolution of these kinks is dominated by a hopping dynamics, related directly to the underlying spatial structure (cf. Fig. 1).

The aim of this paper is to characterize the nondiffusive dynamics of a kink state under the influence of internal noise. The temporal evolution of the kinks is characterized by a hopping dynamic. This dynamic is a result of the combinations of the effects of system size and inherent fluctuations. Figure 1 illustrates this type of dynamic. When the kinks are spatially monotonous the system borders attract exponentially the interfaces. Based on bistable universal models, we characterize the origin of these unexpected dynamics, through determination of the kinematic laws and the survival probability of the kink position. In the case of nonmonotonous kinks, as a result of fluctuations and the system size, the interface exhibits a hopping dynamic. The bistable universal models allow us to characterize the origin of these unexpected dynamics. Numerical simulations show quite good agreement with the theoretical predictions.

The paper is organized as follows. In Sec. II, a prototype model for dissipative bistability systems is considered—the real Ginzburg-Landau equation. The stochastic dynamics exhibited by an interface between two symmetric states is characterized by finding its kinematics law and the survival probability. Interfaces with damped spatial oscillations are analyzed in Sec. III. As a result of fluctuations and the system size, an interface between two symmetric states exhibits a hopping dynamic. Analogously, by obtaining the kinematic law and the survival probability of of the kink position, the hopping dynamic is characterized. Our conclusions and remarks are left to the final section.

II. REAL GINZBURG-LANDAU EQUATION UNDER THE INFLUENCE OF INTERNAL NOISE

The simplest model that describes bistable systems is the supercritical real Ginzburg-Landau equation [38]. This model accounts for the dynamics of a scalar order parameter $u(x,t)$, where $\{x,t\}$ stand for the spatial coordinate and time, respectively. The scalar order parameter satisfies

$$\partial_t u = \mu u - u^3 + \partial_{xx} u, \tag{1}$$

where μ is the control parameter and the last term on the right-hand side accounts for the coupling process between the different local domains, which is of diffusive type. Depending on the context in which this equation has been derived, the physical meaning of the field $u(x,t)$ could be the dominant magnetization, electric field, phytomass density, average molecular orientation, or chemical concentration, to mention a few. For negative μ, the above model is characterized by exhibiting a single equilibrium, $u = 0$. This scenario is modified when the control parameter changes sign. For $\mu > 0$, $u = 0$ is always unstable, while the homogenous states $u = \pm\sqrt{\mu}$ are stable. Hence, this model exhibits bistability.

The above model is variational type, that is,

$$\partial_t u = -\frac{\delta \mathcal{F}[u]}{\delta u},$$

with the Lyapunov function

$$\mathcal{F}[u] = \int \left(\frac{1}{2} (\partial_x u)^2 - \frac{\mu}{2} u^2 + \frac{1}{4} u^4 \right) dx. \tag{2}$$

Therefore, the dynamical behavior of this system consists in the minimization of the functional $\mathcal{F}$, the free energy. Since the homogenous states $u = \sqrt{\mu}$ and $u = -\sqrt{\mu}$ have the same free energy, we expect that an arbitrary initial condition can generate the appearance of domains. That is, solutions that connect regions with different equilibria. One solution that accounts for a single domain is (the Ising wall or kink solution)

$$u_k^{\pm}(x;\Delta) = \pm\sqrt{\mu} \tanh\left[\sqrt{\frac{\mu}{2}} (x - \Delta) \right] \tag{3}$$

where Δ stands for the position separating the different domains, that is, $u_k^{\pm}(x = \Delta) = 0$ and the core of the kink is $l = \sqrt{2/\mu}$. The positive (negative) sign describes the kink (antikink) solution. Figure 2 illustrates the kink solution, its position, and core, respectively.

A. Stochastic real Ginzburg-Landau equation and kink dynamics

To describe the internal inherent fluctuations of the macroscopic system under study, let us consider an additive noise

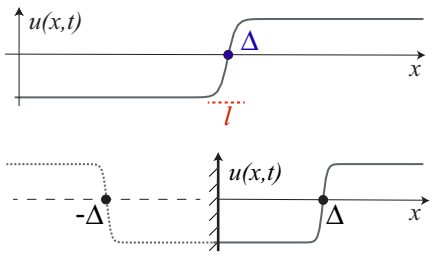

FIG. 2. (Color online) Domain solution between two symmetric states, kink solution (top), $\{\Delta, l\}$ account for the position and the core of the kink. Bottom shows a kink and an antikink solution as consequence of the specular boundary condition.

term in the Ginzburg-Landau equation [38]

$$\partial_t u = \mu u - u^3 + \partial_{xx} u + \sqrt{\eta}\zeta(x,t), \tag{4}$$

where η is the noise intensity level, for equilibrium systems this parameter is proportional to the temperature. $\zeta(x,t)$ is a Gaussian white noise with zero mean value, $\langle \zeta(x,t)\rangle = 0$, and correlation

$$\langle \zeta(x,t)\zeta(x',t')\rangle = \delta(x-x')\delta(t-t'), \tag{5}$$

where parentheses $\langle\ \rangle$ accounts for average over the noise realizations. Then, the noise is spatially and temporally independent.

To determine the effect of fluctuations on the kink solution we consider the noise intensity level as small ($\eta \ll 1$) and the following ansatz

$$u(x,t) = u_k^+(x - \Delta(t)) + w(x,\Delta), \tag{6}$$

where the kink position, $\Delta(t)$, is promoted to a temporal function of the order of η and w is a small corrective function. Introducing the above ansatz in Eq. (4) and linearizing in w, one obtains

$$\mathcal{L}w = \dot{\Delta}\partial_x u_k^+ + \sqrt{\eta}\zeta(x,t), \tag{7}$$

where the linear operator $\mathcal{L} \equiv -\mu + 3(u_k^+)^2 - \partial_{xx}$ is a self-adjoint operator, when one introduces the inner product $(f|g) = \int f(x)g(x)dx$. Besides, this operator satisfies $\mathcal{L}\partial_x u_k^+ = 0$. Hence, to solve the above linear equation we multiply it by $\partial_x u_k^+$, integrating throughout all the space and then we obtain the solvability condition

$$\dot{\Delta} = \sqrt{\bar{\eta}}\bar{\zeta}(t), \tag{8}$$

where $\bar{\eta} \equiv \eta/(\partial_x u_k^+|\partial_x u_k^+)$ and

$$\bar{\zeta}(t) \equiv \frac{\int \zeta(x,t)\partial_x u_k^+ dx}{(\partial_x u_k^+|\partial_x u_k^+)} \tag{9}$$

is a Gaussian white noise with zero mean value, $\langle\bar{\zeta}(t)\rangle = 0$, and correlation

$$\langle\bar{\zeta}(t)\bar{\zeta}(t')\rangle = \delta(t-t'). \tag{10}$$

Therefore, the kink position satisfies a simple Langevin dynamic, Eq. (8), describing a Brownian particle [36,46,47]. The kink position Eq. (8) is derived rigorously in Ref. [48]. Associated with the above Langevin equation, one has the following equation for the conditional probability (Fokker-Planck equation [46,47])

$$\partial_t P(\Delta,t|\Delta_0,t_0) = \frac{\bar{\eta}}{2}\partial_{\Delta\Delta} P(\Delta,t|\Delta_0,t_0), \tag{11}$$

where $P(\Delta, t = t_0|\Delta_0,t_0) = \delta(\Delta - \Delta_0)$. Then, the conditional probability satisfies a simple diffusion equation and its evolution is characterized by the dispersion of a Gaussian. Simulating the above equation in a finite system with absorbing boundary conditions [$P(\Delta = L,t|\Delta_0,t_0) = P(\Delta = 0,t|\Delta_0,t_0) = 0$, where L is the system size], the probability does not conserve its norm and accounts for the survival probability. Notwithstanding, numerical simulations of Eq. (4) for a single kink solution in a finite system with specular boundary conditions do not exhibit this behavior, where the survival probability distribution spreads asymmetrically. Figure 3(a) outlines the evolution of the kink position and its conditional probability. It is important to note that when the kink reaches the border of the system it disappears, because the system minimizes its free energy [cf. Fig. 3(a)]. Then the probability distribution for sufficiently small noise accounts for the survival probability of the kink, i.e., this probability does not preserve its norm. This probability corresponds to the kink remaining within the system. Once it reaches the border the survival probability is no longer considered. In addition, we note that the expected value moves toward the center of the system.

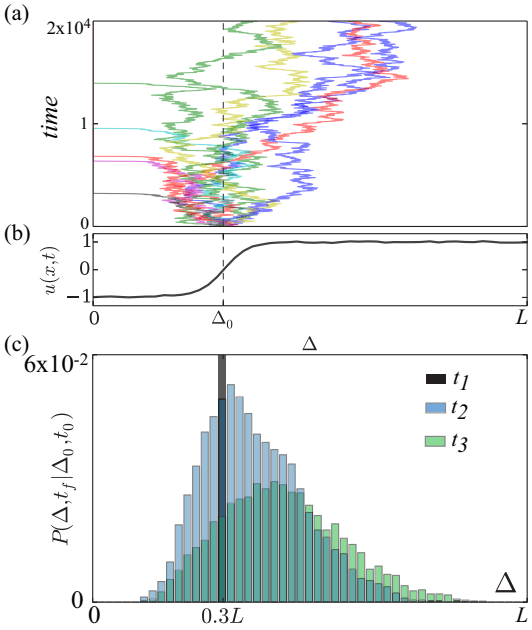

FIG. 3. (Color online) Stochastic dynamics of a kink state. (a) Numerical simulations of a single kink of Eq. (4) in a finite size system with specular boundary conditions, with $\mu = 1$ and $\eta = 0.0018$ and $L = 25$, starting at the position $\Delta = 0.3L$. (b) The profile link at an initial moment. (c) Evolution of survival probability of a single kink for different instants of time, $t_1 = 0$ (black), $t_2 = 20000$ (blue), and $t_3 = 40000$ (green).

B. System size effects

To account for the dynamics described above, one must consider the effects of system size. Thus, we consider the Ginzburg-Landau equation, model (4), in a given domain L with specular or Neumann boundary conditions, i.e., $\partial_x u(x = 0,t) = \partial_x u(x = L,t) = 0$. These boundary conditions are consistent with having an Ising wall as a solution. The effect of boundary conditions is to create mirror images of the kink, so its dynamics is described by considering the system as extended with a kink-antikink pair. Figure 2 illustrates the system size effect. The dynamics of the kink-antikink pair can be described by considering the following ansatz

$$u(x,t) = u_k^+[x + \Delta(t)] + u_k^-[x - \Delta] - \sqrt{\mu} + w(x,\Delta), \quad (12)$$

where the kink position, $\Delta(t)$, is promoted to a temporal variable, the position of the left edge is set in the origin of the coordinate system, and $w(x,\Delta)$ is a small corrective function. Note that the above ansatz is valid when the kink and antikink are sufficiently isolated, i.e., Δ is much larger than the core of the kink ($\Delta \gg l$). Introducing the above ansatz in Eq. (4), linearizing in w, and imposing the solvability condition, in a similar manner to the previous calculation, we obtain the following Langevin equation

$$N\dot{\Delta} = f_1(\Delta) + f_2(\Delta) + f_3(\Delta) + \sqrt{\bar{\eta}}\bar{\zeta}(t)N, \quad (13)$$

where

$$f_1(\Delta) \equiv 3\sqrt{\mu}(\partial_x u_k^- | u_k^-[u_k^+ - \sqrt{\mu}]), \quad (14)$$

$$f_2(\Delta) \equiv 3(\partial_x u_k^- | (u_k^-)^2[u_k^+ - \sqrt{\mu}]), \quad (15)$$

$$f_3(\Delta) \equiv 3(\partial_x u_k^- | u_k^-[u_k^+ - \sqrt{\mu}]^2), \quad (16)$$

and the mobility $N \equiv (\partial_x u_k^- | \partial_x u_k^-)$ is a constant. The above equation describes the kinematic law for the kink position as result of size effect. The dynamics of the kink position has three sources $f(\Delta) = f_1 + f_2 + f_3$. With the aim of to obtain insight into the dynamics, we consider the limit of diluted kink, that is, the domains are sufficiently separated ($\Delta \gg 1/\sqrt{\mu}$). Then, the third term on the right side is negligible, and after straightforward calculations we obtains the following expression

$$\dot{\Delta} = -\alpha e^{-2\sqrt{2\mu}\Delta} + \sqrt{\bar{\eta}}\bar{\zeta}(t), \quad (17)$$

where α is positive constant defined by

$$\alpha \equiv -6\sqrt{\mu}\frac{\int e^{-\sqrt{2\mu}x}[u_k^- + \sqrt{\mu}]u_k^-\partial_x u_k^- dx}{(\partial_x u_k^- | \partial_x u_k^-)}. \quad (18)$$

Therefore, the boundary condition produces an attractive force on the kink, which is exponential with a characteristic length $1/2\sqrt{2\mu}$. To verify the above kinematic law, we follow numerically the evolution of the position and the speed of kink. Figure 4 shows the comparison between the numerical and deterministic kinematic law predicted by the kink-antikink interaction, formula (13) with $\eta = 0$. Here we observe a good agreement between the numerical observations and theoretical predictions. However, when the kinks are closer the interaction intensifies and the exponential law is no longer valid. The analytical description of this dynamic becomes complex and is only accessible numerically. Notice that the range of validity of the kinematic law is $\Delta > \sqrt{2/\mu}$

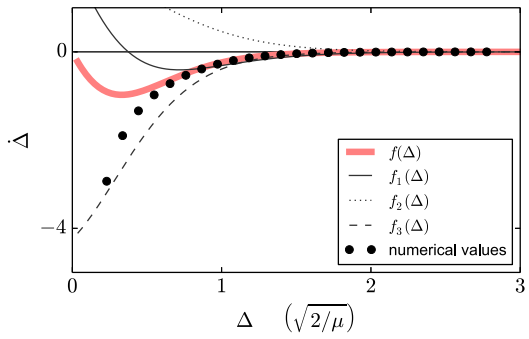

FIG. 4. (Color online) Kinematic law of the kink position as a result of size effect. Points are obtained numerically by considering a uniform distribution of initial conditions for a single kink, then numerically the system evolves during a brief moment of time, and finally the temporal variation of the kink position is calculated. The solid line is the analytical expression (13) with $\eta = 0$, and $f(\Delta) = f_1 + f_2 + f_3$.

To describe the effect of the two edges, one must consider that the kink is under the influence of two antikinks, then the dynamic of a kink in a finite system is described by

$$\dot{\Delta} = h(\Delta) + \sqrt{\bar{\eta}}\bar{\zeta}(t), \quad (19)$$

with $\Delta \leqslant L$ and $h(\Delta) \approx -\alpha e^{-2\sqrt{2\mu}\Delta} + \alpha e^{-2\sqrt{2\mu}(L-\Delta)}$ for large Δ, $\Delta \gg \sqrt{\mu}$ and $(L - \Delta) \gg \sqrt{\mu}$. Thus, each border attracts the kink with an intensity that decays asymptotically in an exponential manner. Associated with this Langevin equation, one has the following Fokker-Planck equation

$$\partial_t P(\Delta,t|\Delta_0,t_0) = -\partial_\Delta [h(\Delta)]\, P + \frac{\bar{\eta}}{2}\partial_{\Delta\Delta} P, \quad (20)$$

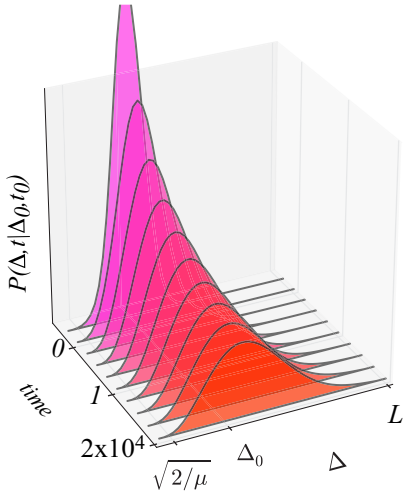

FIG. 5. (Color online) Temporal evolution of Fokker-Plank Eq. (20) with absorbing boundary conditions, using a drift force $h(\Delta) = -C[\Delta^{-a} + (L - \Delta)^{-a}]$ with C=0.033, a=3.08, Δ_0=0.3L, and $\eta = 2.69 \times 10^{-3}$.

with the absorbing boundary conditions $P(\Delta = 0,t|\Delta_0,t_0) = P(\Delta = 0,t|\Delta_0,t_0) = 0$ and $P(\Delta,t|\Delta_0,t_0)$ account for the survival probability of the kink, which was initially at $\Delta = \Delta_0$. These boundary conditions take into consideration that when the kink reaches the border it disappears. Figure 5 shows the evolution of the survival probability, considering a fitting drift force of the form $h(\Delta) = -C[\Delta^{-a} + (L - \Delta)^{-a}]$, where $\{C,a\}$ are fittings parameters. This simple drift force accounts qualitatively for the kinematics law of kink position in whole system, including the dynamic near the borders of the system. The survival probability has qualitative good agreement with the numerical simulations of Eq. (4), see the bottom panel of Fig. 3(c). Therefore, the kink dynamics under the influence of internal noise and system size effects exhibits nondiffusive behavior.

III. NONMONOTONIC KINK SOLUTIONS

One of the main characteristics of the domains between two symmetric states exhibited by the real Ginzburg-Landau equation, model (1), is that the kinks are monotonously increasing or decreasing spatially (see Fig. 2). Several bistable physical systems with symmetric uniform states show interfaces between two states with spatially damped oscillations, nonmonotonic kink solutions. Examples of these fronts are observed in a shallow one-dimensional fluidized granular layer subjected to a periodic air flow [20,21], population dynamics models [24], predator-prey systems [22,49], parametrically driven chain of pendula [50], to mention a few. Figure 6 shows the typical profile of a nonmonotonic kink solution. Because of the spatial oscillations, the size of the kink core is several times larger than in the case of monotonous kink states. Therefore, one expects a more relevant role of interactions between kinks and system border in the dynamics of these interfaces. To understand the dynamics of these nonmonotonic kink solutions, let us consider the simplest model that describes a bistable system with nonmonotonic kink solutions, the Swift-Hohenberg equation

$$\partial_t u = \mu u - u^3 - (\partial_{xx} + q^2)^2 u + \sqrt{\eta}\zeta(x,t), \qquad (21)$$

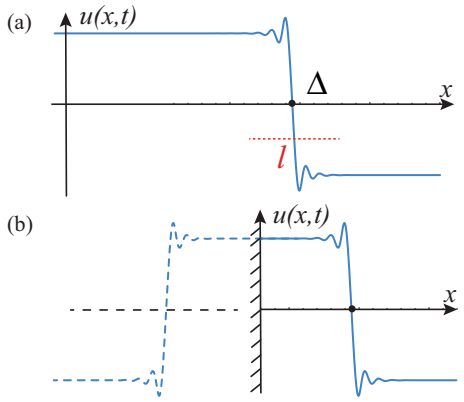

FIG. 6. (Color online) Domain solution between two symmetric states with damping spatial oscillations (top), $\{\Delta,l\}$ account for the position and the core of the kink. Bottom: kink and an antikink solution as consequence of the specular boundary condition.

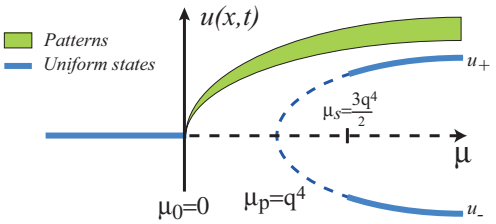

FIG. 7. (Color online) Bifurcation diagram of Swift-Hohenberg Eq. (21), where the darkened area accounts for the amplitude of the patterns. The continuous and dashed lines account for stable and unstable uniform states, respectively. $\{\mu_0,\mu_p\}$ correspond to the spatial and the pitchfork bifurcations of the state $u = 0$, respectively. μ_s stands for the spatial bifurcation of the states $u_\pm = \pm\sqrt{\mu - q^4}$.

where $u(x,t)$ is a scalar field, μ is the bifurcation parameter, q is the pattern wave-number parameter, η is the noise intensity level, and $\zeta(x,t)$ is a Gaussian white noise with zero mean value, $\langle\zeta(x,t)\rangle = 0$, and correlation $\langle\zeta(x,t)\zeta(x',t')\rangle = \delta(x - x')\delta(t - t')$. The Swift-Hohenberg model was introduced to describe the onset of Rayleigh-Benard convection, however, recent generalizations have been used intensively to account for pattern formation in several physical systems [3,4].

The deterministic Swift-Hohenberg Eq. (21), $\eta = 0$, describes a spatial supercritical bifurcation. For $\mu < 0$, the system presents a stable uniform state $u(x,t) = 0$. At $\mu \equiv \mu_0 = 0$ the system bifurcates, the uniform solution becomes unstable and giving rise to a pattern state. For $\mu > 0$, the pattern amplitude, at wave number $k_c = \pm q$, grows as the square root of μ. Figure 7 illustrates the bifurcation diagram of Swift-Hohenberg Eq. (21), where the shaded area stands for the amplitude of the patterns. If one continues to increase the bifurcation parameter μ, the unstable uniform state $u = 0$ has a secondary pitchfork bifurcation for $\mu \equiv \mu_p = q^4$, which generates new uniform unstable states $u_\pm = \pm\sqrt{\mu - q^4}$ (see Fig. 7). These states become stable through a spatial bifurcation, when one increases the bifurcation parameter, at $\mu \equiv \mu_s = 3q^4/2$ [51]. Then for a bifurcation parameter larger than μ_s, one expects to observe kinks between uniform states. Figure 8 shows the typical kink observed in this model. Although nonmonotonous kink solutions, u_k are simple and occur in many dynamical systems, there are not analytical expressions of these solutions. This is due to fact that the kink solutions are solutions of the deterministic stationary system, $\partial_t u = 0$,

$$\mu u_k - u_k^3 - (\partial_{xx} + q^2)^2 u_k = 0, \qquad (22)$$

which is a Lagrangian system with the following action

$$S = \int \left(-\frac{(\mu - q^2)}{2} u_k^2 + \frac{u_k^4}{4} - q^2 (\partial_x u_k)^2 + \frac{(\partial_{xx} u_k)^2}{2} \right) dx. \qquad (23)$$

This system has only one conserved quantity that corresponds to the Hamiltonian function, which has the form

$$E = \frac{(\mu - q^2)}{2} u_k^2 - \frac{u_k^4}{4} - q^2 (\partial_x u_k)^2 + \frac{(\partial_{xx} u_k)^2}{2} - \partial_x u_k \partial_{xxx} u_k. \qquad (24)$$

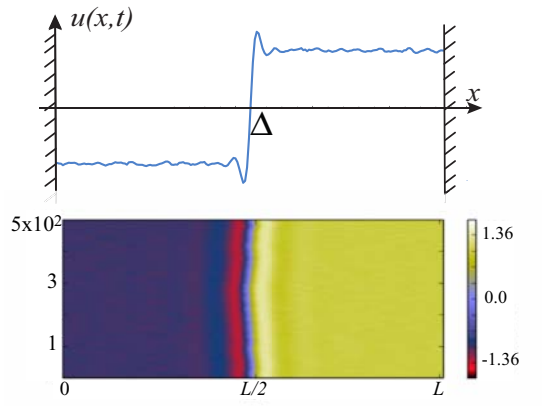

FIG. 8. (Color online) Kink solution of the Swift-Hohenberg equation with the parameters $\mu = q = 1$ and $\eta = 0.0018$. (a) kink solution profile and (b) spatiotemporal evolution of the kink.

Then, the dynamical system is not integrable, and one can show that the kink and localized structures displayed on this stationary dynamical system (22) are the result of chaotic behavior in this system [52].

One can characterize the asymptotic behavior of the kink through linearizing Eq. (22) around uniform states

$$u_k(x \to \pm\infty) \to \pm\sqrt{\mu - q^4}e^{-ax}\cos(bx) + u_{\pm},$$

where $a \equiv \sqrt{2\mu - 3q^4}/4\sqrt{-q^2 + \sqrt{2(\mu - q^4)}}$ and $b \equiv \sqrt{-q^2 + \sqrt{2(\mu - q^4)}}$. Thus, one can analytically characterize the spatial damped oscillations exhibiting nonmonotonic kink solution. It is worth noting that, this type of asymptotic behavior is fundamental to characterize the interaction between kinks.

A. Nondiffusive dynamics of nonmonotonic kink solution under the influence of internal noise and system size effects

We consider the effects of the stochastic term in the kink dynamics of the stochastic Swift-Hohenberg Eq. (21), considering a size domain L with specular boundary conditions. Numerical simulations of this model show that the kink dynamics is not diffusive type. Figure 9 shows different realization of trajectories of the kink position from the same initial condition, the nonmonotonic kink solution at the initial time and the spatiotemporal evolution of the survival probability. Unexpectedly, we observe that the evolution of the kink is characterized by a hopping dynamic. That is, the position of the kink remains for long periods fluctuating around defined positions and suddenly changes its position. It is also important to note that the fluctuations near the border are smaller. From the different trajectories of the kink position, we can build up the survival probability of the kink to remain inside the domain [cf. Fig. 9(c)]. We observe that the distribution initially spreads asymmetrically, similar to the evolution of the survival probability described in the previous section. Subsequently, a local maximum begins to emerge of the survival probability at a precise distance inward from the border of the domain. Later, a local maximum begins to emerge at a given distance to the border of the domain, as it is illustrated

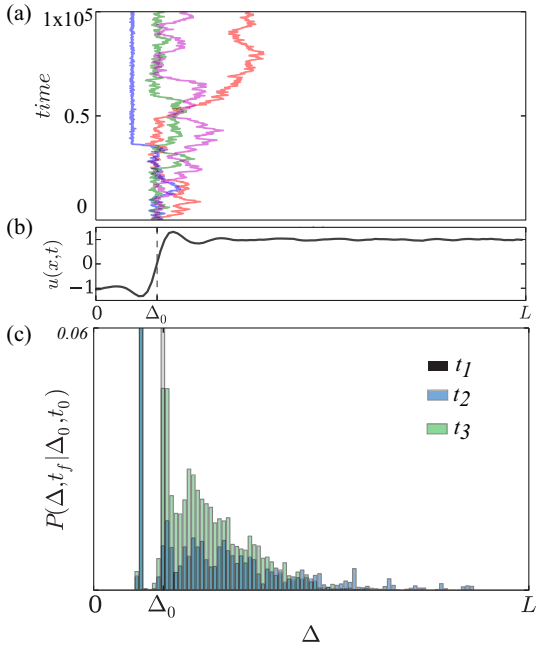

FIG. 9. (Color online) Stochastic dynamics of a kink state of the stochastic Swift-Hohenberg Eq. (21). (a) Numerical simulations of a single kink of the model (21) in a finite size system with specular boundary conditions, with $\mu = 1$, $q = 1$ and $\eta = 0.0018$ starting at the position $\Delta = \Delta_0 \approx 0.15L$. (b) The kink at an initial moment. (c) Evolution of survival probability of a single kink at different instants of time, $t_1 = 0$ (gray), $t_2 = 10^6$ (green), and $t_3 = 2 \times 10^6$ (blue).

in the spatiotemporal evolution of the survival probability [see Fig. 9(c)]. Likewise, as a result of fluctuations is that this type of nonmonotone kink exhibits the appearance of a spatial pattern on the homogeneous states. This phenomenon is due to the fact that the noise is exciting equally all spatial modes, however, the decay rate of the spatial modes are different and the mode with slowest decay rate has a finite wavelength. Thus, the balance between relaxation and fluctuations of the spatial modes generates an incoherent pattern. This phenomenon is known in the literature as precursor [41,53,54]. Notice that the spatial damped oscillations observed on the deterministic nonmonotone kink also result from the spacial slower decay mode. Hence, one expects noise-induced precursors in these kinks. For instance, this was experimentally observed in the granular kinks in a shallow one-dimensional fluidized granular layer subjected to a periodic air flow (cf. Fig. 1).

To understand the intriguing dynamics described above, we will use a similar strategy to the one we have used to figure out the dynamics of the monotonic kink under the influence of internal noise and system size effects. That is, we will consider the dynamics of a kink and an antikink generated by the boundary conditions. Let us consider the ansatz

$$u(x,t) = u_k[x + \Delta(t)] + u_{ak}[x - \Delta(t)] - \sqrt{\mu - q^4} + w(x,\Delta), \quad (25)$$

where u_{ak} stands for an antikink solution, $\Delta(t)$ is the kink position, which has been promoted to a temporal variable, the

position of the left edge is set to the origin of the coordinate system, and $w(x,\Delta)$ is a small corrective function. The above ansatz is valid when the kink and antikink are sufficiently diluted, i.e., Δ is much larger than the kink core ($\Delta \gg 1$). Figure 6(b) shows the solution generated by the above ansatz. Introducing this ansatz in Eq. (21), linearizing in w, and imposing the solvability condition, in a similar manner to the precedent calculations, we obtain the following Langevin equation

$$N\dot{\Delta} = f_1'(\Delta) + f_2'(\Delta) + f_3'(\Delta) + \sqrt{\eta'}\bar{\zeta}(t)N, \tag{26}$$

where

$$f_1'(\Delta) \equiv 3\sqrt{\mu}(\partial_x u_{ak}|u_{ak}[u_k - \sqrt{\mu - q^4}]), \tag{27}$$

$$f_2'(\Delta) \equiv 3(\partial_x u_{ak}|(u_{ak})^2[u_k - \sqrt{\mu - q^4}]), \tag{28}$$

$$f_3'(\Delta) \equiv 3(\partial_x u_{ak}|u_{ak}[u_k - \sqrt{\mu - q^4}]^2), \tag{29}$$

and the mobility $N \equiv (\partial_x u_{ak}|\partial_x u_{ak})$ is a constant. In the limit of diluted kinks, the above dynamics reads

$$\begin{aligned}\dot{\Delta} &= -\frac{\partial U}{\partial \Delta} + \sqrt{\eta'}\bar{\zeta}(t),\\ &= -\alpha' e^{-2a\Delta}\sin(2b\Delta) + \sqrt{\eta'}\bar{\zeta}(t),\end{aligned} \tag{30}$$

where the potential is

$$U(\Delta) \equiv -e^{2a\Delta}\frac{b\cos(2b\Delta) + a\sin(2a\Delta)}{2(a^2+b^2)},$$

α is a constant defined by

$$\alpha' \equiv -\sqrt{\mu - q^4}\frac{\int e^{-ax}\sin(bx)(u_k)^2\partial_x u_k dx}{(\partial_x u_k|\partial_x u_k)}.$$

and $\eta' \equiv \eta/(\partial_x u_k|\partial_x u_k)$.

Therefore, the spatial damped oscillations and the boundary condition produce a force that alternates between being attractive and repulsive. To verify the above kinematic law of the kink position, similarly to what we have presented in the previous section, we have considered a uniform distribution of initial conditions for a single kink, then we numerically evolve the system for a brief moment of time, and finally we calculate the temporal variation of the kink position. Figure 10 depicts the comparison between the numerical and deterministic kinematics law in a similar manner of the previous section. The numerical and theoretical results shows an adequate agreement. However, when the kinks are closer enough the interaction intensifies and the kinematic law is no longer valid. The analytical description of this dynamic becomes complex and is only accessible numerically. Although, the analytical calculation in this region is only valid qualitatively.

From the kinematic law of the kink position, Eq. (30), and its respective potential, we can infer that the system has a family of equilibria, which satisfies approximatively $\sin(2b\Delta^*) = 0$, separated by a constant distance $l = \pi/2b$, i.e., $\Delta_n^* = \pi n/2b$ with $n = 1,2,\ldots$. Notice that the equilibria are more stable as one approaches the system borders. Figure 10 shows the shape of potential $U(\Delta)$ near the system border.

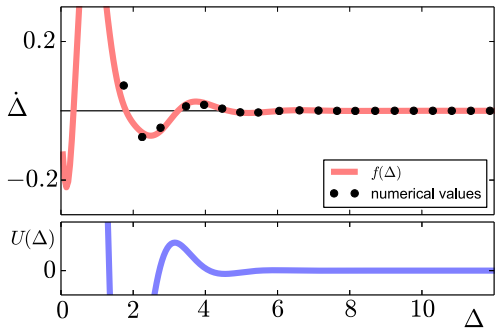

FIG. 10. (Color online) Kinematic law of the kink position as a result of size effect. Points are obtained numerically by considering a uniform distribution of initial conditions for a single kink, then numerically the system evolves in a brief moment of time, and finally the temporal variation of the kink position is calculated. The solid curve is obtained by using the integral form of the kinematic law of the kink position $f(\Delta) = f_1' + f_2' + f_3'$, using the expressions (27–29). The lower panel shows the potential $U(\Delta)$.

The dynamics around a given equilibrium, $\Delta(t) = \Delta^* + v(t)$, takes the form

$$\dot{v} = -\alpha' 2be^{-2a\Delta^*}v + \sqrt{\eta'}\bar{\zeta}(t). \tag{31}$$

Then the dispersion around a given equilibrium take the form

$$\langle v^2\rangle = \frac{\eta'}{\alpha' 2be^{-2a\Delta^*}}.$$

Hence, the fluctuations around more stable equilibria are smaller. That is, one expects the width around an equilibrium of the survival probability to get smaller, when it is closer to the border (cf. bottom panel of Fig. 9). It is important to note that recent observations of the dynamics of granular kinks in a shallow one-dimensional fluidized granular layer subjected to a periodic air flow exhibit similar dynamic behavior that the one described above, that is, these granular kinks show a hopping dynamic [20,21].

From Langevin Eq. (30), one can derive the Fokker-Planck equation for the survival probability of the kink

$$\partial_t P(\Delta,t|\Delta_0,t_0) = \partial_\Delta\left[\frac{\partial U}{\partial \Delta}\right]P + \frac{\eta'}{2}\partial_{\Delta\Delta}P, \tag{32}$$

with the absorbing boundary conditions $P(\Delta = 0,t|\Delta_0,t_0) = P(\Delta = 0,t|\Delta_0,t_0) = 0$. Figure 11 shows the evolution of the survival probability, which has good qualitative agreement with the numerical simulations of the stochastic Swift-Hohenberg Eq. (21). Hence, the kink dynamics under the influence of internal noise and system size effects exhibits nondiffusive behavior with a hopping dynamic.

Due to the boundary conditions, the survival probability for large times converges asymptotically to a zero solution. However, since the system is of potential type, one can easily infer the qualitative behavior of the survival probability. For example, one expects that initially the probability distribution widens asymmetrically, as a result of the nucleation barrier, the distribution grows into the system by exploring the attraction basins of different equilibria, exhibiting new local maxima. Later, the local maxima appearing are those towards the system

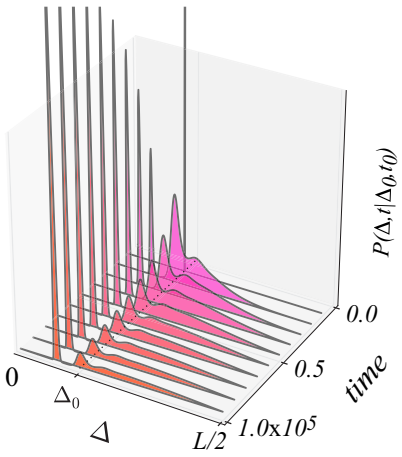

FIG. 11. (Color online) Temporal evolution of Fokker-Plank Eq. (32) with absorbing boundary conditions, using the potential (30) with $\alpha' = 1.157$, $a = 0.4940$, and $b = 1.026$ as fitting parameters and $\eta' = 2 \times 10^{-3}$.

borders, which eventually will become the dominant peaks. Finally, they began to decrease. The above description is consistent with the numerical observations (cf. Fig. 9). It is worthy to note that throughout the presented analysis, we have assumed that the creation of a kink from a large fluctuation of the uniform state is a highly improbable event. Such events are easily observed for high noise levels.

B. Hopping dynamics sustained by inhomogeneities

Other kinks or fronts, which exhibit an interesting hopping dynamic as a consequence of noise are the solutions connecting two periodic states [44]. This phenomenon is evident because pattern states generate a nucleation barrier opposing the propagation of the wall. Therefore this phenomenon is not related to border effects. An alternative way to generate a hopping dynamic, which is not generated by the border effects, is considering that the parameters are spatially modulated. Note that this type of forcing breaks the translational invariance of the system. Since one expects that any particle-type solution will prefer some precise spatial positions, then the presence of noise will generate a hopping dynamic. In order to illustrate this dynamic, let us consider the following forcing real Ginzburg-Landau equation

$$\partial_t u = a\cos(kx) + \mu u - u^3 + \partial_{xx} u + \sqrt{\eta}\zeta(x,t), \qquad (33)$$

where a and k, respectively, are the amplitude and wave number of the forcing. For small forcing, the homogeneous states of the Ginzburg-Landau Eq. (12) become periodic and they have the form $u \approx \pm\sqrt{\mu} - a\cos(kx)/2\mu$. Then, the kink solution of the real Ginzburg-Landau equation [see formula (3)], now connects two periodic states induced by periodic forcing, which are positioned at precise positions of the form $2\pi n/k$, with $n = 1,2,3,\ldots$. Performing an analysis similar to that the one we have implemented in the previous sections, we obtain the following kinematic law for the kink position

$$\dot{\Delta} = \alpha'' \sin(k\Delta) + \sqrt{\bar{\eta}}\bar{\zeta}(t), \qquad (34)$$

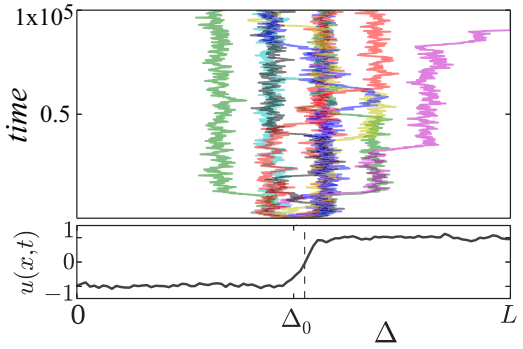

FIG. 12. (Color online) Stochastic dynamics of a kink state of the forcing real Ginzburg-Landau Eq. (33) with $k = \pi/3$, $a = 0.02$, and $\eta = 0.02$. Different colors represent different trajectories of the kink solution. The bottom panel shows the profile of the kink at the initial time.

where $\alpha'' = a\int_{-\infty}^{\infty} \partial_x u_k^+(x)\cos(kx)dx/(\partial_x u_k^+|\partial_x u_k^+)$. Then, the dynamic of the kink position is characterized by a Brownian particle in a periodic potential. Reference [55] presents a detailed analysis of this type of stochastic particle. Figure 12 shows the numerical trajectories of stochastic kink solutions of the forcing real Ginzburg-Landau Eq. (33), where all solutions begin at the same initial condition. Hence, this system clearly exhibits hopping dynamics sustained by inhomogeneities. In the trajectories illustrated in this figure, there are not border effects, as they approach the border the above dynamics is modified by the effects of the interaction with a virtual kink. Note that for small forcing and large noise intensity level, the $u(x,t)$ profile field does not exhibit clear periodic oscillations. However, the forcing effect is evident in the dynamics of the kink.

IV. CONCLUSIONS AND REMARKS

Diverse macroscopic physical systems exhibit spontaneous breaking of symmetry generating extended bistable systems. As a result of the inherent fluctuations, these systems exhibit coexisting domains separated by interfaces or domain walls. Moreover, fluctuations induce an erratic dynamic of the interfaces, which is expected of diffusive nature. However, we show that joint effect of the inherent fluctuations and size effects induces unexpected nondiffusive dynamics of an interface between two symmetric states.

Monotonous kink solutions under the influence of fluctuations are characterized by exhibiting nonsymmetric random walks. These trajectories are characterized by being attracted to the system borders. Hence, the survival probability in a given domain is characterized by a nondiffusive dynamic.

In the particular case of domains between two symmetrical states with damped spatial oscillations, the temporal evolution of these nonmonotonous kinks is characterized by a hopping dynamic. As the interface approaches the borders, the fluctuations decrease and the interface remains longer around well-defined positions. Such dynamic behavior has

been recently observed qualitatively in an interface between two symmetric states in a shallow one-dimensional fluidized granular layer subjected to a periodic air flow, where each domain varies periodically with half the period of the forcing (cf. Fig. 1). A rigorous analysis in this direction a subject for future research.

ACKNOWLEDGMENTS

The authors thank E. Vidal-Henriquez for the critical reading of the manuscript. M.G.C. thanks the financial support of FONDECYT Project 1120320. D.A.C.C. thanks Conicyt fellowship *Beca Nacional*, Contract No. 22131268.

[1] G. Nicolis and I. Prigogine, *Self-Organization in Non Equilibrium Systems* (Wiley, New York, 1977).
[2] L. M. Pismen, *Patterns and Interfaces in Dissipative Dynamics*, Springer Series in Synergetics (Springer, Berlin, 2006).
[3] M. C. Cross and P. C. Hohenberg, Rev. Mod. Phys. **65**, 851 (1993).
[4] M. Cross and H. Greenside, *Pattern Formation and Dynamics in Nonequilibrium Systems* (Cambridge University Press, New York, 2009).
[5] Y. Pomeau, Physica D **23**, 3 (1986).
[6] J. S. Langer, Rev. Mod. Phys. **52**, 1 (1980).
[7] P. Collet and J. P. Eckman, *Instabilities and Fronts in Extended Systems*, Princeton Series in Physics (Princeton University Press, Princeton, 2014).
[8] A. H. Eschenfelder, *Magnetic Bubble Technology* (Springer, Berlin, 1980).
[9] T. Börzsönyi, S. Akamatsu, and G. Faivre, Phys. Rev. E **80**, 051601 (2009).
[10] M. G. Clerc, S. Residori, and C. S. Riera, Phys. Rev. E **63**, 060701 (2001).
[11] D. Gomila, P. Colet, G. L. Oppo, and M. San Miguel, Phys. Rev. Lett. **87**, 194101 (2001).
[12] M. G. Clerc, T. Nagaya, A. Petrossian, S. Residori, and C. Riera, Eur. Phys. J. D **28**, 435 (2004).
[13] S. Residori, Phys. Rep. **416**, 201 (2005).
[14] V. Petrov, Q. Ouyang, and H. L. Swinney, Nature (London) **388**, 655 (1997).
[15] I. Aranson and L. Tsimring, *Granular Patterns* (Oxford University Press, Oxford, 2008).
[16] F. Melo, P. B. Umbanhowar, and H. L. Swinney, Phys. Rev. Lett. **75**, 3838 (1995).
[17] S. Douady, S. Fauve, and C. Laroche, Europhys. Lett. **8**, 621 (1989).
[18] S. J. Moon, M. D. Shattuck, C. Bizon, D. I. Goldman, J. B. Swift, and H. L. Swinney, Phys. Rev. E **65**, 011301 (2001).
[19] S. J. Moon, D. I. Goldman, J. B. Swift, and H. L. Swinney, Phys. Rev. Lett. **91**, 134301 (2003).
[20] J. E. Macias, M. G. Clerc, C. Falcon, and M. A. Garcia-Nustes, Phys. Rev. E **88**, 020201 (2013).
[21] J. E. Macias and C. Falcon, New J. Phys. **16**, 043032 (2014).
[22] J. D. Murray, *Mathematical Biology* (Springer, Berlin, 1989).
[23] R. A. Fisher, Ann. Eugen. **7**, 355 (1937).
[24] M. G. Clerc, D. Escaff, and V. M. Kenkre, Phys. Rev. E **72**, 056217 (2005); **82**, 036210 (2010).
[25] W. van Saarloos and P. C. Hohenberg, Physica D **56**, 303 (1992).
[26] P. Coullet, Int. J. Bifurcation Chaos **12**, 2445 (2002).
[27] A. Kolmogorov, I. Petrovsky, and N. Piskunov, Bull. Univ. Moskou Ser. Int. Se. **7**, 1 (1937).
[28] W. van Saarloos, Phys. Rep. **386**, 29 (2003).
[29] G. Ahlers and D. S. Cannell, Phys. Rev. Lett. **50**, 1583 (1983).
[30] J. Fineberg and V. Steinberg, Phys. Rev. Lett. **58**, 1332 (1987).
[31] T. R. Powers and R. E. Goldstein, Phys. Rev. Lett. **78**, 2555 (1997).
[32] J. Langer, in *Solids Far from Equilibrium*, edited by C. Godrèche (Cambridge University Press, Cambridge, 1992).
[33] S. Residori, A. Petrossian, T. Nagaya, C. Riera, and M. G. Clerc, Physica D **199**, 149 (2004).
[34] R. E. Goldstein, G. H. Gunaratne, L. Gil, and P. Coullet, Phys. Rev. A **43**, 6700 (1991).
[35] P. Coullet, J. Lega, B. Houchmanzadeh, and J. Lajzerowicz, Phys. Rev. Lett. **65**, 1352 (1990).
[36] W. Horsthemke and R. Lefever, *Noise-Induced Transitions: Theory and Applications in Physics, Chemistry and Biology* (Springer, Berlin, 1984).
[37] L. Gammaitoni, P. Hänggi, P. Jung and F. Marchesoni, Rev. Mod. Phys. **70**, 223 (1998).
[38] J. Garcia-Ojalvo and J. M. Sancho, *Noise in Spatially Extended Systems* (Springer-Verlag, New York, 1999).
[39] G. Agez, P. Glorieux, M. Taki, and E. Louvergneaux, Phys. Rev. A **74**, 043814 (2006).
[40] M. G. Zimmermann, R. Toral, O. Piro, and M. San Miguel, Phys. Rev. Lett. **85**, 3612 (2000).
[41] G. Agez, M. G. Clerc, and E. Louvergneaux, Phys. Rev. E **77**, 026218 (2008); G. Agez, M. G. Clerc, E. Louvergneaux, and R. G. Rojas, *ibid.* **87**, 042919 (2013).
[42] L. Q. Zhou, X. Jia, and Q. Ouyang, Phys. Rev. Lett. **88**, 138301 (2002).
[43] R. Muller, K. Lippert, A. Kuhnel, and U. Behn, Phys. Rev. E **56**, 2658 (1997).
[44] M. G. Clerc, C. Falcon, and E. Tirapegui, Phys. Rev. Lett. **94**, 148302 (2005); Phys. Rev. E **74**, 011303 (2006).
[45] Experimental image of a granular kink and temporal evolution of kink position is a courtesy of J. Macias and C. Falcon.
[46] N. G. V. Kampen, *Stochastic Process in Physics and Chemistry* (North-Holland, Amsterdam, 1992).
[47] C. Gardiner, *Handbook of Stochastic Methods* (Springer-Verlag, Berlin, 1985).
[48] T. Funaki, Prob. Th. Rel. Flds. **102**, 221 (1995).
[49] S. R. Dunbar, J. Math. Biol. **17**, 11 (1983).
[50] M. G. Clerc, S. Coulibaly, and D. Laroze, Int. J. Bifurcation Chaos **19**, 3525 (2009).
[51] A. Hagberg, A. Yochelis, H. Yizhaq, C. Elphick, L. Pismen, and E. Meron, Physica D **217**, 186 (2006).
[52] P. Coullet, C. Elphick, and D. Repaux, Phys. Rev. Lett. **58**, 431 (1987).
[53] G. Agez, C. Szwaj, E. Louvergneaux, and P. Glorieux, Phys. Rev. A **66**, 063805 (2002).
[54] W. Schöpf and W. Zimmermann, Phys. Rev. E **47**, 1739 (1993).
[55] H. Risken, *Fokker-Planck Equation* (Springer, Berlin, 1984).